Numerical simulation of angular structure of the near-horizon sky brightness in ground-based observations. Part 1. The aerosol atmosphere

T.B. Zhuravleva, I.M. Nasretdinov, and S.M. Sakerin

Institute of Atmospheric Optics, Siberian Branch of the Russian Academy of Sciences, Tomsk

Received January 15, 2003

Calculations by the method of adjoint walks are used to study the effect of atmospheric sphericity and vertical stratification of aerosol optical characteristics on angular distribution of near-horizon clear-sky brightness in ground-based observations. It is shown that, for small aerosol optical depths and/or large solar zenith angles, the neglect of atmospheric sphericity may introduce up to 10% error in radiance calculations. The specific feature of near-horizon sky brightness is that it depends not only on the atmospheric optical depth, but also on aerosol extinction coefficient in the near-ground layer. To cope with this it is sufficient to use meteorological visibility as accurate as 50%.

Introduction

Theoretical and experimental studies of the spatial distribution of clear-sky brightness (see, e.g., Refs. 1–6) have improved significantly our understanding of the processes of solar radiative transfer in the atmosphere. The relationships derived have made it possible to develop the methods of solution of inverse problems and, in particular, the methods of determination of aerosol optical characteristics from scattered radiation in the solar almucantar (as described in Refs. 6–13 among others).

Use of specialized solar photometer of Aerosol Robastic Network (AERONET) system (http://spamer.gsfc.nasa.gov) has increased substantially the information content of approaches based on measurements of diffuse radiation in solar almucantar. With the advent of modern computer technologies and development of the corresponding mathematical means (see, e.g., Refs. 14 and 15), the network measurements can now be used for retrieving aerosol scattering phase function, aerosol microstructure, refractive index, and single scattering albedo in different regions of the Earth. The latter two characteristics are especially important in view of the recently increased attention to the problem of aerosol radiative forcing.

The solution of direct and inverse problems was successful for ground-based observations of daylight clear sky, and much less successful for near-horizon sky regions that are still insufficiently investigated experimentally[16] and theoretically.[17,18] At the same time, preliminary analysis of the problem has shown that study of the field of incident radiation at large (larger than 75°) zenith angles, in context of the problems on the visibility of remote objects and sky brightness backgrounds in horizon regions may have promising results. With regard to the inverse problems, the aerosol optical characteristics can, in principle, be reconstructed using approaches analogous to those developed for almucantar experimental geometry. A common feature of these two different tasks (dealing with solar almucantar and region of horizon) is that they both use as the initial information the azimuth dependence of scattered radiation at a constant zenith angle. At the same time, they mainly differ in that the angular structure of near-horizon sky brightness is determined primarily by aerosol optical properties in the near-ground layer rather than vertically integrated column characteristics obtained in solar almucantar observations. As an example, Reference 19 illustrates the possibility of using near-horizon method and describes, for a particular case, the algorithm of determination of single scattering albedo in the IR spectral range.

The ultimate goal of our study is to develop few-parameter models of clear-sky daylight near-horizon sky brightness for use in interpreting ground-based observations, suitable to solve a range of direct and inverse problems. In this paper, we propose an efficient algorithm of calculation of brightness field of near-horizon solar radiation (without the account for molecular absorption), and present estimates of the effect of atmospheric sphericity and vertical stratification of aerosol optical characteristics on angular distribution of intensity obtained. A more general case, which takes into account the atmospheric gaseous absorption, will be addressed in the second part of the paper.

1. Statement of the problem

We consider a plane parallel atmospheric model, and assume that unidirectional flux of solar radiation is incident on the top of the atmosphere along the direction $\boldsymbol{\omega}_0 = (\xi_0, \varphi_0)$, where ξ_0 and φ_0 are solar zenith and azimuth angles, respectively (Fig. 1). Solution of monochromatic radiative transfer equation (with indices λ for a wavelength not displayed) for

0235-6880/03/05–06 496-09 $02.00

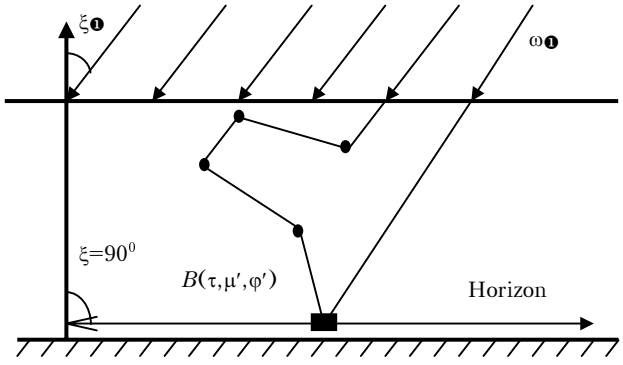

Fig. 1. Illumination geometry in the model of plane parallel atmosphere.

sensing along a horizontal direction $\boldsymbol{\omega}_H = (\xi = 90°, \varphi)$ at the surface level reads as follows[4,19]:

$$B_H(\tau,\varphi) = S(\tau,\mu=0,\varphi) = \frac{\kappa}{\varepsilon}B^0(T_{atm}) + \\ + \frac{\Lambda_0}{4\pi}\int_{\varphi'=0}^{2\pi}\int_{\mu'=-1}^{1} g(\mu=0,\mu')B(\tau,\mu',\varphi')\,d\mu'd\varphi'. \qquad (1)$$

Here τ is the atmospheric optical depth (aerosol extinction plus molecular scattering); $\varepsilon = \kappa + \sigma$ are the extinction, absorption, and scattering coefficients; $\Lambda_0 = \sigma/\varepsilon$ is the single scattering albedo of the molecular plus aerosol atmosphere; $g(\mu,\mu')$ is the scattering phase function; $S(\tau,\mu,\varphi)$ is the source function; $B^0(T_{atm})$ is the Plank's function at atmospheric temperature T_{atm}; $B(\tau, \mu', \varphi')$ is the sky and surface brightness "illuminating" the observation path.

Because the intrinsic atmospheric emission $B^0(T_{atm})$ in shortwave spectral range is low, we can neglect the first term in Eq. (1), and write the second term as a sum of two components, describing single scattering of direct solar radiation $B_{\odot}$ within the solid angle $\Omega_{\odot}$ and multiple scattering by the atmosphere and underlying surface:

$$B_H(\tau,\varphi) = B_{H0}(\tau,\varphi) + B_{Hm}(\tau,\varphi) = \\ = \frac{\omega_0}{4\pi}\left[B_{\odot}\, g(\mu=0,\mu_{\odot})\,\Omega_{\odot} + \right. \\ \left. + \int_{\varphi'=0}^{2\pi}\int_{\mu'=-1}^{1} g(\mu=0,\mu')B_m(\tau,\mu',\varphi')\,d\mu'd\varphi'\right], \qquad (2)$$

where $B_{\odot} = B_{\odot 0}\exp(-\tau m)$, $B_{\odot 0}$ is the extraterrestrial spectral solar constant; and m is the optical air mass along the direction toward the sun. This expression gives a clear idea of how much every component contributes to the brightness B_H of the sky observed at the horizon. From Eq. (2) it follows that the multiple-scattering component B_m is most difficult to describe correctly. This means that the method chosen must separate the single and multiple scattering contributions to the intensity of radiation incident on the receiver.

2. Atmospheric model

The scattered radiation field is frequently studied using the model of plane parallel atmosphere proposed to solve many direct and inverse problems of atmospheric optics. However, in a number of cases, the scattering and absorption processes can be described correctly only if atmospheric sphericity is taken adequately into account; in particular, this is the case in problems dealing with the observations of daytime horizon from space or with twilight atmospheric sensing. The calculations of daylight near-horizon clear-sky brightness fields, performed assuming that observer is at the surface, also should take into account the sphericity of the atmosphere.[18]

Consider a coordinate system XYZ whose origin O coincides with the center of the Earth (Fig. 2). A parallel solar flux $\boldsymbol{\omega}_{\odot} = (-1, 0, 0)$ is incident on the top of the atmosphere, assumed to be a sphere of the radius R_{atm}, along the direction opposite to OX-axis.

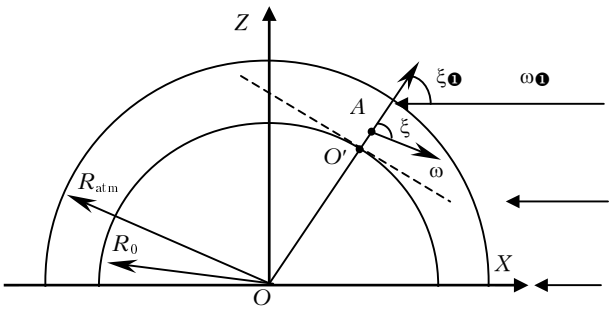

Fig. 2. Model of the spherical atmosphere.

The distribution density in the YZ plane is assumed to be equal to $1/\pi R_{atm}^2$. (A "single particle" is incident on the entire top of the atmosphere; and a total amount of radiant energy, incident on the planet with radius R_{atm} per unit time, is $\pi R_{atm}^2\,\pi S$, where πS is the solar constant). The observer is at the point A with coordinates $\mathbf{r}^* = (x^*, 0, z^*)$. The angular distribution of incoming radiation at the point A is defined in local rectangular coordinate system with the origin at O', the point of intersection of OA-axis with the Earth's surface of radius R_0; in this coordinate system, there is the axis OA, and azimuth angle is measured from the XOZ-axis. In this local coordinate system, the position of observer is characterized by the coordinates $(0, 0, h)$, $h \ll (R_{atm} - R_0)$; and the direction of incident solar radiation and viewing direction are given by the vectors $\boldsymbol{\omega}_{\odot} = (\xi_{\odot}, \varphi_{\odot} = 180°)$ and $\boldsymbol{\omega} = (\xi, \varphi)$, respectively. Here, $\xi_{\odot}$ and ξ are the angles the vectors $\boldsymbol{\omega}_{\odot}$ and $\boldsymbol{\omega}$ make with OA-axis, while the angle $\varphi = 0$ corresponds to the viewing direction toward the sun.

The vertically inhomogeneous atmospheric model will be considered to have piecewisely constant structure, divided into N spherical layers with the boundaries (R_i, R_{i+1}), $R_i = R_0 + H_i$, $i = 1, ..., N$, $R_N = R_{atm}$, each with constant values of all optical characteristics. If we let h denote the height above the Earth's surface, then for $H_{i-1} \le h \le H_i$, $i = 1, ..., N$, the optical atmospheric model will be described as follows:

– aerosol extinction coefficients

$$\varepsilon_{aer,i}(h) = \varepsilon_{aer,i};$$

– aerosol scattering coefficients

$$\sigma_{aer,i}(h) = \sigma_{aer,i};$$

– aerosol absorption coefficients

$$\kappa_{aer,i}(h) = \kappa_{aer,i};$$

– aerosol single scattering albedo

$$\Lambda_{aer,i}(h) = \Lambda_{aer,i};$$

– molecular (Rayleigh) scattering coefficients

$$\sigma_{R,i}(h) = \sigma_{R,i};$$

– molecular absorption coefficients

$$\kappa_{mol,i}(h) = \kappa_{mol,i};$$

– aerosol scattering phase function

$$g_{aer,i}(\mu, \mu', h) = g_{aer,i}(\mu, \mu').$$

In most of the calculations presented here, the vertical stratification of aerosol extinction coefficient was either represented by an exponential distribution, adequately describing the mean profiles $\varepsilon_{aer}(h)$:

$$\varepsilon_{aer}(h) = \varepsilon_{aer}(0) \exp(-\beta h), \qquad (3)$$

or by the aerosol models recommended by World Climate Research Programme (WCP).[20] Recall that, in accordance with Ref. 20, the atmosphere 30 km in depth is divided into 4 layers, each with aerosol characteristics assumed constant (Table 1). The vertical profile of Rayleigh scattering was considered to follow the exponential distribution[21]:

$$\sigma_R(h,\lambda) = \left(\frac{\lambda_0}{\lambda}\right)^4 \sigma_R(h,\lambda_0),$$

$$\sigma_R(h, \lambda_0) = \sigma_R(0) \exp(-0.125h),$$

$$\sigma_R(0) = 0.0119 \text{ km}^{-1}, \lambda_0 = 0.55 \text{ μm}.$$

The underlying surface will be assumed to reflect according to Lambert law and have albedo A_s.

At this stage of problem solution, the effect of refraction will be neglected.

3. Solution technique

The spatial and angular characteristics of solar radiation under clear-sky conditions can be calculated by different methods; for a comprehensive overview and comparative analysis of techniques see, e.g., Ref. 4. The algorithms of Monte Carlo method are most important of them because they can easily take into account the characteristics of real atmosphere, use any reasonable number of detectors without significant loss of computation efficiency, discriminate single and multiple scattered components of diffuse radiation, etc.

Let us consider the brightness of scattered radiation at the observation point $\mathbf{r}^*$, averaged over the solid angle Ω_1

$$B(\mathbf{r}^*, \boldsymbol{\omega}_1) = \int_{\Omega_1} B(\mathbf{r}^*, \boldsymbol{\omega})\, d\boldsymbol{\omega}.$$

The angle Ω_1 is defined by the viewing direction $\boldsymbol{\omega}_1 = (\xi, \varphi_1)$ and aperture angle 2γ, $0 < \gamma < \pi/2$; γ is measured from $\boldsymbol{\omega}_1$. When *azimuthal* dependence of incident radiation is studied for specified coordinates of observation point $\mathbf{r}^*$ and viewing zenith angle ξ in the aerosol-molecular atmosphere, the most efficient method of calculation of $B(\mathbf{r}^*, \boldsymbol{\omega}_k)$, $\boldsymbol{\omega}_k = (\xi, \varphi_k)$, $k = 1, 2, ..., N_\varphi$, is the method of adjoint walks (MAW).

According to the MAW ideology (see, e.g., Ref. 18), the brightness falling within the angle Ω_1 and recorded with a detector is given as

$$B(\mathbf{r}^*, \boldsymbol{\omega}_1) = M\xi,$$

Table 1. Vertical profiles of aerosol optical characteristics recommended by WCP[20] at $\lambda = 0.55$ μm

Height interval, km	Aerosol		
	Urban	Continental	Marine
0–2	$\varepsilon_{aer} = 0.5$ km^{-1}, $\tau_{aer} = 1$, $\Lambda_{aer} = 0.647$	$\varepsilon_{aer} = 0.1$ km^{-1}, $\tau_{aer} = 0.2$, $\Lambda_{aer} = 0.891$	$\varepsilon_{aer} = 0.05$ km^{-1}, $\tau_{aer} = 0.1$ $\Lambda_{aer} = 0.989$
2–12	$\varepsilon_{aer} = 0.0025$ km^{-1}, $\tau_{aer} = 0.025$, $\Lambda_{aer} = 0.891$		
12–20	$\varepsilon_{aer} = 0.218 \cdot 10^{-3}$ km^{-1}, $\tau_{aer} = 0.1744 \cdot 10^{-2}$, $\Lambda_{aer} = 1$		
20–30	*Background stratospheric aerosol* ε_{aer} (20 km) $= 0.218 \cdot 10^{-3}$ km^{-1}, ε_{aer} (30 km) $= 0.332 \cdot 10^{-4}$ km^{-1}, for ε_{aer} (20–30 km) a linear interpolation is used, $\Lambda_{aer} = 1$		

where $M\xi$ is the mathematical expectation of random variable $\xi = \sum_{n=0} \eta(\mathbf{r}_n, \mathbf{w}_n)$. To estimate $B(\mathbf{r}^*, \boldsymbol{\omega}_1)$, it is necessary:

– to simulate backward trajectories from point $\mathbf{r}^*$ with directions distributed uniformly over Ω_1, i.e., with the density $\delta(\mathbf{r} - \mathbf{r}^*)/|\Omega_1|$,

– to calculate $\eta_n(\mathbf{r}_n, \mathbf{w}_n)$ at each collision point $\mathbf{r}_n$ (here, $\mathbf{w}_n$ is the direction of particle motion before collision at point $\mathbf{r}_n$).

In the plane atmospheric model (identified by subscript *pp*) the quantity $\eta_n = \eta_n^{\text{pp}}(\mathbf{r}_n, \mathbf{w}_n)$ is defined by the formula

$$\eta_n^{\text{pp}}(\mathbf{r}_n, \mathbf{w}_n) = 0.5\Lambda(\mathbf{r}_n)\exp\left[-\tau(\mathbf{r}_n)\right] g(\mathbf{w}_n, -\mathbf{w}_0)|\Omega_1| .$$

Here, $\Lambda(\mathbf{r}_n)$ is the single scattering albedo at the point $\mathbf{r}_n$; $\tau(\mathbf{r}_n)$ is the optical path from point $\mathbf{r}_n$ to the top of the atmosphere along the $-\boldsymbol{\omega}_0$ direction; $g(\mathbf{w}_n, -\boldsymbol{\omega}_0)$ is the scattering phase function of the medium at the point $\mathbf{r}_n$. Because of the axial symmetry of the sun–atmosphere–earth system, the contribution to intensity can be calculated simultaneously for a set of viewing directions $\boldsymbol{\omega}_k$, $\boldsymbol{\omega}_k = (\xi, \varphi_k)$, $k = 1, 2, ..., N_\varphi$, by simulating a single photon trajectory along the direction $\boldsymbol{\omega}_1 = (\xi, \varphi_1)$. For this, in calculating the η_n^{pp} estimate it is necessary to change from a given direction of solar radiation incidence, $\boldsymbol{\omega}_0$, to a set of variable directions $\boldsymbol{\omega}_{0,k} = (a_{0,k}, b_{0,k}, c_{0,k})$, $k = 1, 2, ..., N_\varphi$, with the coordinates

$$a_{0,k} = \sin\xi_0 \cos(\varphi_0 + \varphi_1 - \varphi_k);$$

$$b_{0,k} = \sin\xi_0 \sin(\varphi_0 + \varphi_1 - \varphi_k);$$

$$c_{0,k} = -\cos\xi_0.$$

In the model of spherical atmosphere (subscript *sph*), the quantities to be calculated at each point of collision $\mathbf{r}_n$ are represented as

$$\eta_n^{\text{sph}}(\mathbf{r}_n, \mathbf{w}_n) = \Lambda(\mathbf{r}_n)\exp\left[-\tau(\mathbf{r}_n)\right] g(\mathbf{w}_n, -\mathbf{w}_0)|\Omega_1| \Big/ \left(2\pi^2 R_{\text{atm}}^2\right).$$

To check the correctness of the algorithm implementation, we compared our data with the results calculated by other authors. Table 2 presents the intensity of incoming solar radiation ($\mu < 0$) calculated by finite-difference method, *FN*-method,[4] and by the method of adjoint walks (our calculations). The test calculations were performed assuming plane parallel atmosphere for the optical model of urban aerosol (see Table 1). Overall, the three methods seem to satisfactorily agree: the relative difference is within the Monte Carlo computation error. (We note that the relative error of our calculations does not exceed 1% in most cases). The only discrepancy is found for the forward scattering peak ($\mu = \mu_0 = -0.5$), possibly due to the use of different discretization techniques (see Ref. 4 for a more detail).

Let us compare the estimates of angular intensity distribution, obtained by the method of adjoint walks in the model of spherical atmosphere with the isotropic scattering and exponential altitudinal distribution of extinction coefficient $\varepsilon(h)$.[17] Table 3 presents calculations of the horizon brightness B_{H} for different solar zenith angles (SZAs) and two viewing directions, $\varphi = 0$ and 180°. The observed differences in the intensities of diffuse radiation do not exceed 10%, and are, seemingly, caused by inaccuracy of calculations presented in Ref. 17: their relative error is approximately 10%.

The efficiency of calculation algorithm, which is determined by the computer time needed for achieving a given accuracy, depends substantially on complexity of the atmospheric model used. Therefore, in what follows we will consider how strongly the sphericity of the Earth's atmosphere and vertical behavior of the aerosol optical characteristics influence the angular structure of incoming radiation.

Table 2. Comparison of calculated intensity of the scattered radiation incident on the Earth's surface along the direction $\omega = (\xi,\varphi)$ (plane parallel atmospheric model). Input parameters: molecular optical depth $\tau_{\text{R}} = 0.1$, SZA $\xi_0 = 60°$, $A_{\text{s}} = 0$

$\cos\xi = \mu$	$\varphi = 0°$			$\varphi = 90°$			$\varphi = 180°$		
	Finite-difference method[4]	*FN*-method[4]	Method of adjoint walks (our calculations)	Finite-difference method[4]	*FN*-method[4]	Method of adjoint walks (our calculations)	Finite-difference method[4]	*FN*-method[4]	Method of adjoint walks (our calculations)
0.0	0.1252	0.1229	0.1228	0.0343	0.0331	0.0332	0.0258	0.0249	0.0251
–0.1	0.1875	0.1868	0.1866	0.0451	0.0448	0.0448	0.0326	0.0324	0.0326
–0.2	0.2735	0.2725	0.2722	0.0555	0.0552	0.0552	0.0391	0.0388	0.0390
–0.25	–	0.3229	0.3217	–	0.0598	0.0597	–	0.0416	0.0418
–0.3	0.3776	0.3759	0.3745	0.0637	0.0637	0.0636	0.0440	0.0439	0.0441
–0.4	0.4716	0.4915	0.4934	0.0694	0.0692	0.0691	0.0469	0.0467	0.0470
–0.5	0.6884	0.6853	6.9960	0.0725	0.0748	0.0725	0.0476	0.0495	0.0478
–0.6	0.4733	0.4853	0.4835	0.0740	0.0739	0.0739	0.0473	0.0473	0.0474
–0.7	0.3591	0.3588	0.3580	0.0749	0.0747	0.0749	0.0468	0.0468	0.0471
–0.75	–	0.3046	0.3035	–	0.0750	0.0751	–	0.0469	0.0470
–0.8	0.2563	0.2555	0.2536	0.0755	0.0754	0.0754	0.0474	0.0472	0.0473
–0.9	0.1702	0.1696	0.1690	0.0763	0.0762	0.0763	0.0505	0.0501	0.0505
–1.0	0.0771	0.0775	0.0773	0.0775	0.0775	0.0773	0.0771	0.0775	0.0773

Table 3. Comparison of the horizon brightness in the model of spherical atmosphere, calculated by the method of adjoint walks for $A_s = 0.8$, optical depth $\tau = 0.1$, and single scattering albedo $\Lambda = 1$

SZA ξ_0	Results of Ref. 17		Our calculations	
	$\varphi = 0°$	$\varphi = 180°$	$\varphi = 0°$	$\varphi = 180°$
30	0.0142	0.0154	0.0161	0.0159
60	0.0108	0.01	0.0115	0.0112
80	0.00677	0.00591	0.00636	0.00585
82	0.00601	0.00507	0.0056	0.00499
84	0.00444	0.00352	0.0047	0.00399
86	0.00329	0.00261	0.00365	0.00277
87	0.00281	0.00183	0.00305	0.00209
88	0.00215	0.00147	0.00241	0.00139
89	0.00179	0.000846	0.00176	0.000775

All calculations presented below have been performed for the aerosol optical characteristics corresponding at the wavelength $\lambda = 0.55$ μm, viewing zenith angle $\xi = 89°$, and surface albedo $A_s = 0.2$. The aperture of the receiver ($2\gamma = 0.1°$) is chosen such that there is no single-scattering contribution from the underlying surface.

4. Influence of the atmospheric sphericity on the brightness field of incoming radiation

The effect of atmospheric sphericity on radiative characteristics is usually estimated by comparing (high-accuracy) solutions of radiative transfer equation for spherical and plane parallel geometries. This is rather well explored issue for problems of twilight ground-based atmospheric sensing and satellite study of spatial-angular distribution of the radiation intensity. Whereas for clear-sky ground-based daytime observations the influence of atmospheric sphericity in solar almucantar is well studied, in the near-horizon region the tests are performed just in few cases (e.g., see Refs. 17 and 18 and the bibliography therein).

We performed a series of calculations of the intensity $B(\mu, \varphi)$ of scattered radiation in a wide variability range of the aerosol optical depths $0 \le \tau_{aer} \le 0.9$ and SZAs $0 \le \xi_0 \le 85°$ in spherical and plane atmospheric models. The brightness calculations are more convenient for interpreting in terms of the scattering angle (by analogy with the scattering phase function); therefore, the notation $B(\mu, \varphi)$ will be replaced below by $B(\theta) = B(\mu, \varphi)$, where the scattering angle θ is related to the viewing azimuth angle φ and zenith angles ξ and ξ_0 in the local coordinate system by the formula

$$\cos\theta = \sin\xi \sin\xi_0 \cos\varphi + \cos\xi \cos\xi_0.$$

Obviously, for φ varying in the range $0 \le \varphi \le \pi$, the corresponding range of the angle θ is $(|\xi - \xi_0|, \xi + \xi_0)$.

We characterize the atmospheric sphericity by the quantity

$$\Delta_{sph} = 100\% \frac{B^{sph}(\theta) - B^{pp}(\theta)}{B^{sph}(\theta)}.$$

From comparison it follows that, for small aerosol optical depths ($\tau_{aer} \le 0.05$) and/or large SZAs ($\xi_0 \ge 82°$), the $|\Delta_{sph}|$ values reach 10% (Fig. 3). This means that the neglect of atmospheric sphericity may lead to misunderstanding of specific features of near-horizon brightness field and misinterpretation of the field data. Therefore, all calculations discussed below are performed within the model of spherical atmosphere.

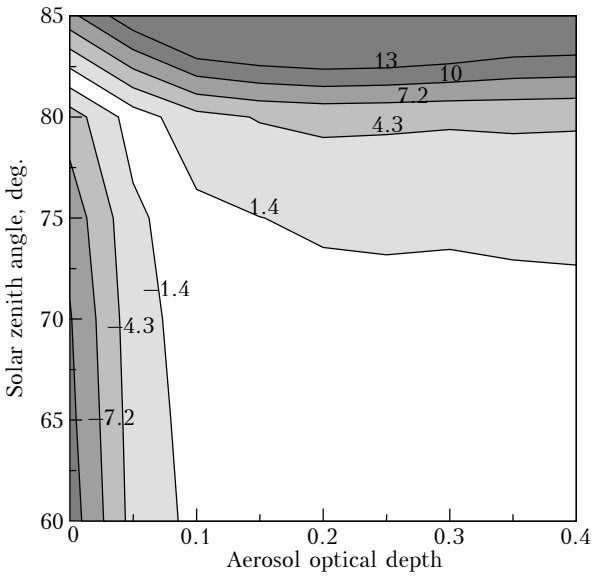

Fig. 3. Relative difference of angular distributions of diffuse radiation Δ_{sph} (%), calculated using the models of spherical and plane-parallel atmosphere.

5. Influence of vertical variations of aerosol optical characteristics

The problem of influence of vertical stratification of aerosol optical characteristics was discussed earlier in context of measurements of diffuse radiation in solar almucantar (in Ref. 3 for direct problems, and in Ref. 14 for inverse problems). It was shown that, within the applicability limits of the model of plane-parallel atmosphere (i.e., for SZAs $\xi_0 \le 75–80°$), the brightness is determined by the integrated optical characteristics of the entire atmospheric column, leading to substantial simplification of the problem solution. In the following sections we will consider how the situation changes in passing to near-horizon viewing angles.

5.1. Vertical profile of aerosol extinction coefficient

From Eq. (2) it follows that the single scattering along a horizontal direction B_{H0} is determined by the single scattering phase function of the atmosphere at

level $h \ll (R_{atm} - R_0)$, and that this function consists of two components:

$$g(\mu = 0, \mu', h) = K_{aer}(h)\, g_{aer}(\mu = 0, \mu', h) + \\ + K_R(h)\, g_R(\mu = 0, \mu', h),$$

$$K_{aer}(h) = \frac{\sigma_{aer}(h)}{\sigma_{aer}(h) + \sigma_R(h)}, \qquad (4)$$

$$K_R(h) = \frac{\sigma_R(h)}{\sigma_{aer}(h) + \sigma_R(h)}.$$

Therefore, the angular distribution of diffuse radiation $B(\theta)$ in the near-horizon region of the sky can be expected to depend on the optical properties of the near-ground layer and the dependence is stronger with increasing of single scattering contribution $B_0(\theta)$ to $B(\theta)$. We performed a numerical experiment to check up this expectation.

Let us consider a model of the atmosphere 30 km in depth. In the height interval 12–30 km we will use the model of stratospheric aerosol (see Table 1), whereas in the layer 0–12 km we will choose four vertical profiles of aerosol extinction coefficient (Fig. 4):

(*a*) $\varepsilon_{aer}(h)$ = const (a vertically homogeneous atmosphere);

(*b*) a two-layer model of $\varepsilon_{aer}(h)$, recommended by WCP for continental conditions (see Table 1);

(*c*) exponential distribution [formula (3)];

(*d*) inverse (parabolic) aerosol distribution within the layer 0–2 km, and $\varepsilon_{aer}(h)$ = const in the layer 2–10 km.

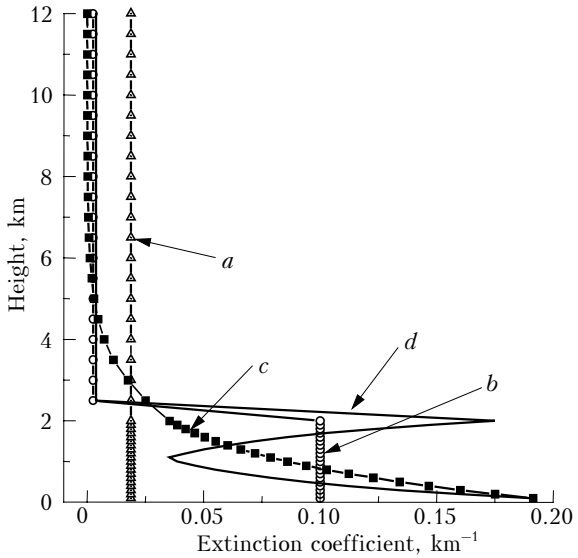

Fig. 4. Profiles of aerosol extinction coefficient in the altitude range from 0 to 12 km: model of vertically homogeneous atmosphere (*a*); model of two-layer atmosphere, by WCP (*b*); exponential distribution (*c*); and inverse aerosol distribution (*d*).

Influence of the type of vertical profile $\varepsilon_{aer}(h)$ on the brightness field will be quantified in terms of

$$\Delta_{pr}(\theta) = 100\% \frac{B^{exp}(\theta) - B(\theta)}{B^{exp}(\theta)},$$

$$\Delta_{pr}^0(\theta) = 100\% \frac{B_0^{exp}(\theta) - B_0(\theta)}{B_0^{exp}(\theta)}.$$

The superscript exp indicates calculations using exponential distribution of aerosol extinction coefficient. The exponential profile $\varepsilon_{aer}(h)$ is chosen as benchmark because it fits the most general tendency of vertical aerosol distribution. Obviously, for an unambiguous $\varepsilon_{aer}(h)$ description, it is sufficient to specify the optical depth τ_{aer} and $\varepsilon_{aer}(0)$ [formula (3)]. The $B^{exp}(\theta)$ calculations are made using detailed vertical grid, with the step of 0.1 km in the interval 0–2 km and with the step of 0.5 km in the interval 2–12 km, for SZA $\xi_0 = 60°$.

In the first numerical experiment, we will compare the calculated results on the brightness with vertical aerosol profiles *a*, *b*, and *c*. The parameters of the distributions *a* and *c* are chosen such that the aerosol optical depth in the height interval 0–12 km is the same for all three distributions and corresponds to the model of continental aerosol with $\tau_{aer} = 0.23$ and $\varepsilon_{aer}(0) = 0.2$ km^{-1}.

Figure 5 presents the calculated data on scattered radiation intensity $B(\theta)$ and its single-scattering component $B_0(\theta)$ for distributions *a*, *b*, and *c*, as well as the quantities $\Delta_{pr}(\theta)$ and $\Delta_{pr}^0(\theta)$. The main feature of $\Delta_{pr}(\theta)$ and $\Delta_{pr}^0(\theta)$ variations is the presence of a pronounced angular behavior (especially for $\Delta_{pr}^0(\theta)$), qualitatively echoing that of the aerosol scattering phase function $g_{aer}(\theta)$. As follows from expression (4), for any fixed viewing angle, $B_0(\theta)$ depends not only on $g_{aer}(\theta)$ and $g_R(\theta)$ values, but also on the weighting factors determined primarily by aerosol extinction coefficient in the near-ground layer. Because aerosol scattering phase function is elongated in the forward direction, $B_0(\theta)$ is dominated by aerosol component of the atmosphere when viewed along the direction toward the sun and by molecular component along the opposite direction.

The maximum differences of brightness fields are found in comparison with vertically homogeneous atmospheric model, primarily for $B_0(\theta)$: $\Delta_{pr}^0(\theta)$ ranges approximately from 20 to –100% as viewing azimuth angle varies from 0 to 180°. In this case, $\varepsilon_{aer}(0)$ values differ by an order of magnitude (see Fig. 4), while parameter $K_{aer}(h = 0)$ is ≈ 0.95 for exponential profile $\varepsilon_{aer}(h)$ and ≈ 0.7 for the profile $\varepsilon_{aer}(h)$ = const. This means that the near-horizon sky brightness is more sensitive to aerosol component in the model with exponential distribution of the extinction coefficient.

The vertical profile $\varepsilon_{aer}(h)$ in the two-layer atmosphere model *b* is more suitable for calculations of near-horizon brightness field: $|\Delta_{pr}(\theta)| \le 5$–7% over the entire range of scattering angles despite the fact

that, as viewing azimuth angle grows, $\Delta^0_{pr}(\theta)$ increases approximately to –20%. This is because the models with vertical profiles *b* and *c* have closer $\varepsilon_{aer}(0)$ values and, hence, closer weighting coefficients $K_{aer}(h = 0)$.

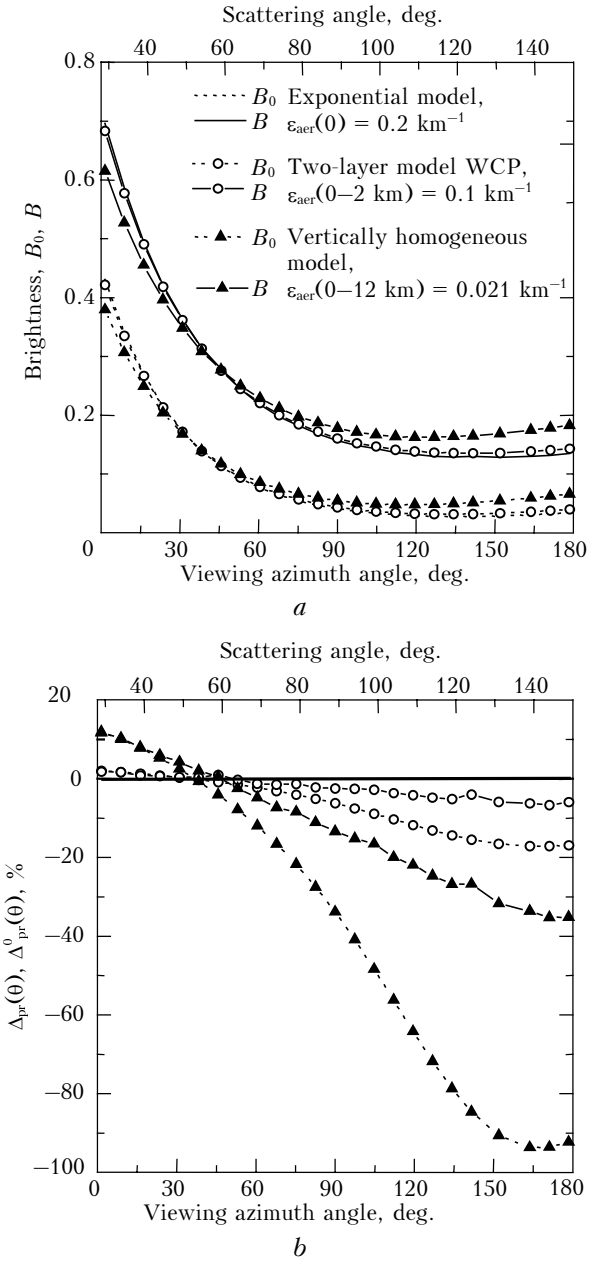

Fig. 5. Angular dependences of diffuse radiation *B* and single-scattering component B_0 (*a*) and their relative differences $\Delta_{pr}(\theta)$ and $\Delta^0_{pr}(\theta)$, calculated for profiles of aerosol extinction coefficient in models *a*, *b*, and *c* (*b*).

Thus, for an adequate treatment of the angular distributions of incoming radiation, the aerosol extinction coefficient in the near-ground layer $\varepsilon_{aer}(0)$ should also be taken into account in addition to the optical depth. In the following numerical experiment we estimate the accuracy of specifying $\varepsilon_{aer}(0)$, which is traditionally determined using meteorological visibility range

$$S_m \approx 3.91/\varepsilon(0). \quad (5)$$

Consider sky brightness for the true $\varepsilon_{aer}(0)$ value of 0.2 km^{-1} which corresponds to $S_m \approx 20$ km, typical in atmospheric haze situations. Suppose that the meteorological visibility is determined accurate to within 50%, such that $10 \le S_m \le 30$ km. How strongly do $B(\theta)$, $B_0(\theta)$, and $B_m(\theta)$ values, calculated for $\varepsilon_{aer}(0) = 0.143$ km^{-1} ($S_m \approx 30$ km) and $\varepsilon_{aer}(0) = 0.35$ km^{-1} ($S_m \approx 10$ km), diverge from the corresponding characteristics for true $\varepsilon_{aer}(0)$?

This deviation will be quantified in terms of the quantity

$$\Delta_{S_m} = 100\% \frac{B(\theta, S_m = 20\,\text{km}) - B(\theta, S_m = S'_m)}{B(\theta, S_m = 20\,\text{km})},$$
$$S'_m = 10; 30\,\text{km}. \quad (6)$$

(The deviations for single- and multiple-scattering components $B_0(\theta)$ and $B_m(\theta)$ are calculated in the same way). As seen from Fig. 6, Δ_{S_m} does not exceed 3–4% over the entire angular range; while the relative difference in calculations of single-scattering component $\Delta^0_{S_m}$ is maximum (≈ –8%) in antisolar directions. In this range, the accuracy of $\varepsilon_{aer}(0)$ specification has minor influence on $B_m(\theta)$: $\left|\Delta^m_{S_m}\right| \le 2 - 3\%$ over the entire range of scattering angles θ. Analogous Δ_{S_m} estimates were obtained for other true τ_{aer} and S_m values.

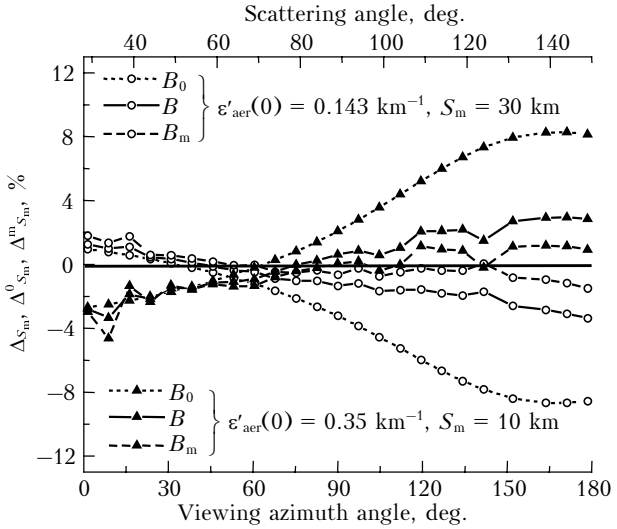

Fig. 6. Relative deviations of brightness, calculated for different $\varepsilon_{aer}(0)$; true value of $\varepsilon_{aer}(0)$ is 0.2 km^{-1}, and $S_m = 20$ km.

Additional numerical experiments indicate that there is no need in assigning exponential $\varepsilon_{aer}(h)$ behavior throughout the altitude range from 0 to 12 km. If $\varepsilon_{aer}(h)$ is defined by formula (3) within lower two-kilometer layer, and $\varepsilon_{aer}(h) = \text{const}$ is assumed in the height interval $2 < h < 12$ km, the relative

deviations of $B(\theta)$, $B_0(\theta)$, and $B_m(\theta)$ will not exceed 1–2%. Now, how will the situation change if inverse aerosol distribution is used instead of the exponential profile $\varepsilon_{aer}(h)$ within the layer 0–2 km (see Fig. 4)? The calculations showed that, for a fixed $\varepsilon_{aer}(0)$ and optical depth $\tau_{aer}(0–2\ \text{km}) = 0.23$, the relative difference in $B(\theta)$, $B_0(\theta)$, and $B_m(\theta)$ does not exceed 2%.

Thus, even if in the near-ground layer the aerosol turbidity is determined inaccurately and an inversion is present, the brightness fields are calculated with quite a reasonable accuracy on the basis of exponential profile $\varepsilon_{aer}(h)$.

5.2. Vertical profile of aerosol single scattering albedo

For analysis of the effect of vertical $\Lambda_{aer}(h)$ stratification, we shall consider two-layer model:

$$\Lambda_{aer}(h) = \begin{cases} \Lambda_1, & 0 \le h < 2\ \text{km} \\ \Lambda_2, & 2 \le h < 12\ \text{km}. \end{cases}$$

Comparison of brightness calculations made for a preset Λ_1 and different Λ_2 values (Fig. 7) has shown that the variations of single scattering albedo in the layer $h > 2$ km have a minor effect on $B(\theta)$, $B_0(\theta)$, $B_m(\theta)$: the relative difference of calculated results does not exceed 2%.

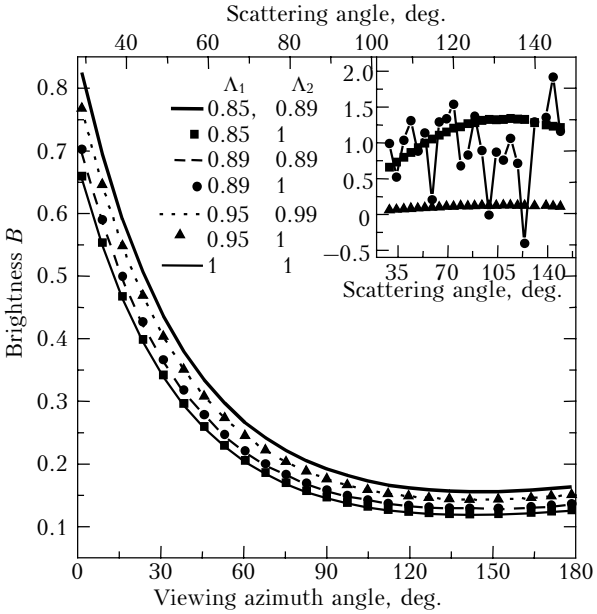

Fig. 7. Influence of profiles of single scattering albedo Λ_{aer} on the near-horizon sky brightness.

Conclusion

To study sky brightness at large viewing zenith angles, we used the method of adjoint walks that allowed us to calculate efficiently the angular structure of incoming solar radiation, including the account of the vertical inhomogeneity of the atmosphere, with the possibility of separating multiple-scattering contribution and generalization to include absorption by atmospheric gases.

Analysis of near-horizon sky brightness calculations has demonstrated that atmospheric sphericity should be taken into account. When the model of plane parallel atmosphere is used for small aerosol optical depths ($\tau_{aer} \le 0.05$) and/or large solar zenith angles ($\xi \ge 82°$), up to 10% errors may result in the brightness determination.

The numerical simulation results indicate that, at large zenith angles, the incoming radiation is determined not only by atmospheric optical depth, but also by the aerosol extinction coefficient in the near-ground layer. To specify $\varepsilon_{aer}(0)$, it is sufficient to use approximate values of meteorological visibility range S_m: even if S_m is estimated with 50% error for typical atmospheric hazes, the relative difference in brightness $B(\theta)$ does not exceed 5%. Thus, from the viewpoint of computation efficiency, in the layer 0–12 km the model of vertical stratification $\varepsilon_{aer}(h)$ should be defined as follows: exponential distribution (with estimated value $\varepsilon_{aer}(0)$) in the height interval 0–2 km and a homogeneous layer in altitude range 2–12 km.

Acknowledgments

The work was supported by Russian Foundation for Basic Research (Grant 02–05–64492).

References

1. K.S. Shifrin and N.P. Pyatovskaya, *Tables of Slant Visibility and Daylight Sky Brightness* (Gidrometeoizdat, Leningrad, 1959), 210 pp.
2. V.V. Sobolev, *Light Scattering in Planetary Atmospheres* (Nauka, Moscow, 1972), 335 pp.
3. G.Sh. Livshits, *Light Scattering in the Atmosphere* (Nauka, Alma-Ata, 1965), 177 pp.
4. J. Lenoble ed., *Radiative Transfer in Scattering and Absorbing Atmospheres: Standard Computational Procedures* (A Deepak Publishing, 1985).
5. V.I. Kushpil, *Clear-sky Daylight Sky Brightness (Experimental Data)* (ONTI GOI, Leningrad, 1971), 164 pp.
6. E.V. Pyaskovskaya-Fesenkova, *Study of Light Scattering in the Earth's Atmosphere* (Publishing House of USSR Academy of Sciences, Moscow, 1957), 219 pp.
7. G.Sh. Livshits and V.E. Pavlov, *Atmospheric Transmission and Relationship between Certain Optical Parameters* (Nauka, Alma-Ata, 1968), pp. 59–64.
8. V.S. Antyufeev, and M.A. Nazaraliev, *Inverse Problems of Atmospheric Optics* (Computer Center of Siberian Branch of the USSR Academy of Sciences, Novosibirsk, 1988), 156 pp.
9. V.A. Smerkalov, *Applied Atmospheric Optics* (Gidrometeoizdat, St. Petersburg, 1997), 334 pp.
10. O.T. Dubovik, T.V. Lapyonok, and S.L. Oshchepkov, Appl. Opt. **34**, No. 36, 8422–8436 (1995).
11. T. Nakajima, G. Tonna, R. Rao, P. Boi, Y. Kaufman, and B. Holben, Appl. Opt. **35**, No. 15, 2672–2686 (1996).
12. C. Devaux, A. Vermeulen, J.L. Deuze, P. Dubuisson, M. Herman, and R. Senter, J. Geophys. Res. **103**, No. D8, 8753–8761 (1998).

13. P. Romanov, N.T. O'Neill, A. Royer, and B.L.J. McArthur, Appl. Opt. **38**, No. 36, 7305–7320 (1999).
14. O. Dubovik, B. Holben, Y. Kaufman, M. Yamasoe, A. Smirnov, D. Tanre, and I. Slutsker, J. Geophys. Res. **103**, No. D24, 31903–31923 (1998).
15. O.T. Dubovik and M. King, J. Geophys. Res. **105**, No. D16, 20673–20696 (2000).
16. V.I. Korzov and L.B. Krasil'shchikov, Tr. Gl. Geofiz. Obs., Issue **275**, 184–194 (1972).
17. G.I. Marchuk, ed., *Monte Carlo Method in Atmospheric Optics* (Nauka, Novosibirsk, 1976), 283 pp.
18. M.A. Nazaraliev, *Statistical Modeling of Radiative Processes in the Atmosphere* (Nauka, Novosibirsk, 1990), 226 pp.
19. S.M. Sakerin, Atmos. Oceanic Opt. **14**, No. 8, 598–601 (2001).
20. *A preliminary cloudless standard atmosphere for radiation computation.* World Climate Research Programme. WCP-112, WMO/TD N 24. 1986. 60 p.
21. G.I. Marchuk and G.A. Mikhailov, Izv Akad. Nauk SSSR, Ser. Fiz. Atmos. Okeana **III**, No. 4, 394–401 (1967).